



Published in final edited form as:

ACS Infect Dis. 2019 July 12; 5(7): 1231–1238. doi:10.1021/acsinfecdis.9b00071.

Antibacterial Activity and Mode of Action of a Sulfonamide-Based Class of Oxaborole Leucyl-tRNA Synthetase Inhibitors

Yuanyuan Si[‡], Sneha Basak[‡], Yong Li[‡], Jonathan Merino[‡], James N. Iuliano[‡], Stephen G. Walker[§], and Peter J. Tonge^{#,†,‡,*}

[#]Center for Advanced Study of Drug Action, John S. Toll Drive, Stony Brook University, Stony Brook, New York 11794, USA

[‡]Department of Chemistry, John S. Toll Drive, Stony Brook University, Stony Brook, New York 11794, USA

[†]Department of Radiology, John S. Toll Drive, Stony Brook University, Stony Brook, New York 11794, USA

[§]Department of Oral Biology and Pathology, John S. Toll Drive, Stony Brook University, Stony Brook, New York 11794, USA

Abstract

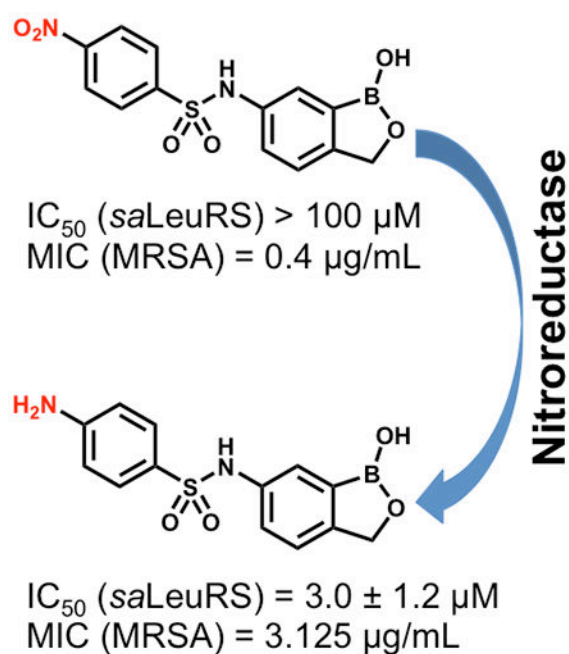
Benzoxaboroles are a class of boron-containing compounds with a broad range of biological activities. A subset of benzoxaboroles have antimicrobial activity due primarily to their ability to inhibit leucyl-tRNA synthetase (LeuRS) via the oxaborole tRNA trapping mechanism, which involves formation of a stable tRNA^{Leu}-benzoxaborole adduct in which the boron atom interacts with the 2'- and 3'-oxygen atoms of the 3'-terminal tRNA adenosine. We sought to identify other antibacterial targets for this promising class of compounds by means of mode of action studies, and we selected a nitrophenyl sulfonamide-based oxaborole (**PT638**) as a probe molecule because it had potent antibacterial activity (MIC of 0.4 µg/mL against methicillin-resistant *Staphylococcus aureus*) but did not inhibit LeuRS (IC₅₀ > 100 µM). Analogues of **PT638** were synthesized to explore the importance of the sulfonamide linker and the impact of altering the functionalization of the phenyl ring. These structure-activity relationship studies revealed that the nitro substituent was essential for activity. To identify the target for **PT638**, we raised resistant strains of *S. aureus* and whole genome sequencing revealed mutations in *leuRS*, suggesting that the target for this compound was indeed LeuRS, despite the lack of enzyme inhibition. Subsequent analysis of **PT638** metabolism demonstrated that bacterial nitroreductases readily converted this compound into the amino analogue, which inhibited LeuRS with an IC₅₀ of 3.0 ± 1.2 µM demonstrating that **PT638** is thus a prodrug.

Graphical Abstract

* Author to whom correspondence should be addressed. Peter J. Tonge: Department of Chemistry, Stony Brook University, Stony Brook, NY 11794-3400, Tel: (631) 632-7907; Fax: (631) 632-6706; peter.tonge@stonybrook.edu.

Supporting Information

Supporting information contains IC₅₀ plots, sequence alignment of the LeuRS proteins from various bacteria, and the synthetic procedures and characterization data for the 6-substituted benzoxaboroles.



Keywords

LeuRS; oxaborole; nitroreductase; nitro prodrug; *S. aureus*; resistance

Multidrug-resistant bacteria are a major threat to human health because they cause infections that are hard to treat and often life-threatening.^{1,2} Drug resistance arises by a variety of mechanisms, including conversion of a drug into inactive metabolites, modification of drug binding sites, changes in cell permeability or drug efflux, and the formation of bacterial populations, such as biofilms, that are less susceptible to antibiotics.^{3,4} One particularly problematic pathogen is methicillin-resistant *Staphylococcus aureus* (MRSA), which is resistant to numerous antibiotics, including most β -lactams,⁵ macrolides, fluoroquinolones, and aminoglycosides.⁶ The threat posed by multidrug-resistant pathogens such as MRSA underscores the need to develop antibiotics with novel mechanisms of action.

The benzoxaboroles are a versatile class of small molecules with potential utility as antibiotics because their selectivity and specificity can be tuned by minor structural modifications. Targets for these compounds include β -lactamases,⁷ PDE4 nucleotide phosphodiesterase,⁸ ROCK kinase,⁹ carbonic anhydrase,¹⁰ and leucyl-tRNA synthetase (LeuRS).¹¹ The oxaborole scaffold can reversibly form covalent tetrahedral complexes with nucleophiles such as hydroxyl groups owing to the presence of the heterocyclic boron atom, which acts as a Lewis acid because it has an empty p orbital.^{12,13} Formation of such complexes is involved in LeuRS inhibition, which occurs via the oxaborole tRNA trapping (OBORT) mechanism (Figure 1), whereby the boron atom forms a tetrahedral complex with both hydroxyl groups of the ribose diol of the terminal 3' tRNA adenosine. Enzyme inhibition via the formation of an enzyme–substrate adduct is also observed in other drug classes, such as the bacterial enoyl-ACP reductases, which are inhibited by isoniazid and

diazaborines.^{14,15} Anacor Pharmaceuticals has developed a number of oxaborole-based inhibitors of LeuRS from bacteria, fungi, protozoa, and other pathogens (Figure 1). **AN2690**,¹¹ which has broad-spectrum antifungal activity, is one of the most effective US Food and Drug Administration–approved treatments for onychomycosis,¹⁶ while **AN6426** is an inhibitor of the *Mycobacterium tuberculosis* LeuRS (minimum inhibitory concentration, MIC 0.13 μ M, *M. tuberculosis* LeuRS IC₅₀ 0.09 μ M),¹⁷ which also has antimalarial activity,¹⁸ and inhibits the growth of *Cryptosporidium* and *Toxoplasma*.^{19,20} Finally, **AN3365**, an aminomethylbenzoxaborole, binds to the editing site of *Escherichia coli* LeuRS with an IC₅₀ value of 0.31 μ M and has broad-spectrum activity against Gram-negative pathogens (MIC 0.5–4 μ g/mL).^{21,22}

Given the good drug-like properties of the oxaborole scaffold and given that both laboratory and clinical isolates show resistance to LeuRS-based inhibitors (arising mainly from mutations in the LeuRS editing domain),^{23,24} we sought to identify new antibacterial targets for this promising class of compounds. Building on the extensive medicinal chemistry efforts conducted by Anacor, we identified the nitrophenylsulfonyl-substituted 6-aminobenzoxaborole **PT638** as a probe molecule (Figure 1). This compound was previously reported to have a MIC value of < 0.2 μ g/mL against *S. aureus* but to not inhibit LeuRS (IC₅₀ > 200 μ M).²⁵ We conducted structure–activity relationship (SAR) studies to explore the importance of the nitro group, sulfonamide linker region, and oxaborole ring for biological activity. These studies revealed that the nitro group was essential for activity. However, whole genome sequencing of resistant bacterial strains suggested that this compound did in fact target LeuRS, despite the lack of enzyme inhibition. Investigation of the mode of action of **PT638** revealed that this compound is reduced to the active species by nitroreductases in MRSA cells.

Results and Discussion

SAR for inhibition of bacterial growth

We began by determining the antibacterial activity of **PT638** toward MRSA (ATCC BAA-1762) and found that the MIC was 0.4 μ g/mL (Table 1). Similarly, we assessed the cytotoxicity of **PT638** to Vero cells using an MTT assay and determined the IC₅₀ to be 100 μ g/mL (Table 1). We subsequently performed SAR studies by synthesizing three series of **PT638** analogues; specifically, we introduced modifications to the substituent on the phenyl ring (SAR1), to the sulfonamide linker (SAR2), and to the oxaborole ring (SAR3) and determined the antibacterial activity of the analogues, as well as their ability to inhibit *S. aureus* LeuRS (saLeuRS) (Figure 2, Table 1).

With the SAR1 analogues, we explored the importance of the 4-nitro group for antibacterial activity (Figure 2). We expected that a strongly electron-withdrawing group like the nitro group would be required for activity, and, in fact, removing the nitro group (**PT649**) or replacing it with an electron-donating methyl group (**PT637**) or methoxy group (**PT661**) did lead to 10-, 100-, and >250-fold increases in MIC, respectively. However, neither replacement of the 4-nitro group with another electron-withdrawing group such as a cyano moiety (**PT657**, MIC >100 μ g/mL) nor relocation of the nitro group to the 2-position

(**PT659**, MIC 6.25 $\mu\text{g}/\text{mL}$) restored the activity to that of the parent compound. When we replaced the 4-nitro group with various 4-halogen atoms, we found that increasing the size of the halogen atom decreased the antibacterial activity: specifically, the 4-fluoro (**PT636**), 4-chloro (**PT651**), and 4-bromo (**PT654**) analogues had MICs of 12.5, 100, and >100 $\mu\text{g}/\text{mL}$, respectively. However, even the most active analogue (4-fluoro) had a MIC value that was 30-fold higher than that of **PT638**. In addition, activity did not depend on the position of the fluorine atom: the 2-fluoro (**PT660**) and 3-fluoro (**PT653**) analogues had MICs similar to that of **PT636**. Other substituents were also explored, but none of the resulting analogues, including 3-fluoro-4-nitro analogue **PT650** and 4-amino analogue **PT662**, were as active as **PT638**. Collectively, these data attest to the critical importance of the 4-nitro group for antibacterial activity.

We subsequently explored the contributions of the sulfonamide linker and the oxaborole ring with the analogues in the SAR2 and SAR3 series, respectively (Figure 2). We found that regardless of whether the phenyl ring carried a 4-nitro or 4-fluoro substituent, replacement of the sulfonamide linker with an amine or amide linker substantially reduced antibacterial activity. All three linker analogues are able to adopt similar, although not identical conformations, while replacement of the sulfonyl moiety with a carbonyl (amide) or methylene (amine) group reduces the number of hydrogen bond acceptors at this position to 1 and 0, respectively (Figure S1). Thus, either the change in geometry and/or alteration in hydrogen bonding propensity may perturb binding to the target. In addition, the oxaborole ring was also critical for activity, as expected for molecules that might exert their activity via the OBORT mechanism; replacement of the oxaborole ring with a lactone (**PT664**) or a boronic acid group (**PT663**) dramatically reduced the activity.

Time-kill experiments and post-antibiotic effect of **PT638**

To further assess the antibacterial activity of **PT638**, we conducted time-kill experiments and determined the duration of the post-antibiotic effect following removal of the test compound from the medium. Treatment of MRSA cells with **PT638** at concentrations 1, 4, and 16 times the MIC led to 1.8 \log_{10} , 2.2 \log_{10} , and 2.7 \log_{10} cfu/mL reductions in cell numbers over 8 h, respectively (Figure 3A). That is, **PT638** showed bacteriostatic activity over the course of 8 h, as indicated by the fact that the cfu reduction was $<3 \log_{10}$.^{26–28} In addition, the duration of the post-antibiotic effect due to the treatment of **PT638** increased from 0.2 h at $0.25 \times \text{MIC}$ to 1.5 h at $4 \times \text{MIC}$ (Figure 3B). However, no further increase in the duration of post-antibiotic effect was observed above $4 \times \text{MIC}$, perhaps because this concentration was sufficient to saturate the target.

Inhibition of saLeuRS and target identification

Next, we used an aminoacylation assay to determine the ability of compounds with MICs of <10 $\mu\text{g}/\text{mL}$ to inhibit saLeuRS. In agreement with previous reports, our data clearly show that **PT638** did not inhibit saLeuRS ($\text{IC}_{50} > 100$ μM , Table 1). In addition, other nitro-substituted analogues, such as **PT659** and **PT650**, also did not inhibit saLeuRS; and **PT649**, which lacks any substituents, showed only weak activity ($\text{IC}_{50} = 94 \pm 2$ μM). In contrast, the 2-fluoro analogue (**PT660**) and the 4-amino analogue (**PT662**) had better activity than **PT638**, with IC_{50} values of 28 ± 1 and 3.0 ± 1.2 μM , respectively (Table 1, Figure S2).

The potent cellular activity of **PT638** combined with its inability to inhibit saLeuRS suggested that it might have some other target in MRSA. To assess this possibility, we generated resistant mutants by plating MRSA (ATCC BAA-1762) on Mueller–Hinton agar plates containing **PT638** at 10 times the MIC. Colonies were obtained with a single-step selection of resistant strains. The frequency of resistance was determined to be 1.5×10^{-8} . Three colonies were picked and were shown to have MICs of $3.125 \mu\text{g/mL}$, which is at least 8 times the MIC of the parent strain. Genomic DNA was extracted, purified, and subjected to whole genome sequencing. However, in each case, the only mutations found were within the *leuRS* gene; the mutations were D343Y, G303S, and F233I, all of which are within the editing domain of saLeuRS (Table 2). Sequence alignment revealed that these three residues are conserved in various pathogens (Figure S3) and that the counterparts of D343 in *E. coli*, *Streptococcus pneumoniae*, and *M. tuberculosis* are directly involved in binding the oxaborole inhibitors.^{17,22,29,30} The other two residues, F233 and G303, are not located in the binding pocket, and it is less clear how mutation of these residues leads to **PT638** resistance. Nevertheless, our results clearly pointed to saLeuRS as the target for **PT638**, which led us to hypothesize that a metabolite of **PT638** might be the cellular inhibitor of saLeuRS.

Activation of prodrug **PT638** by bacterial nitroreductases

Previous studies have shown that bacteria contain nitroreductases, such as NfsA and NfsB, that can reduce a variety of nitroheterocyclic compounds.³¹ For example, the antibacterial agent nitrofurantoin undergoes a reduction that is required for its activity against *E. coli*.³² Enzymatic reduction of nitroaromatic compounds proceeds through a one- or two-electron mechanism³³ in which the nitro group is reduced to an amine via nitroso and hydroxylamine intermediates.^{33,34} On the basis of this previous research, we hypothesized that **PT638** might in fact be a prodrug that needs to be activated by one or more nitroreductases in MRSA (Figure 4A). To test this hypothesis, we evaluated the metabolism of **PT638** following incubation with MRSA cell lysate for 48 h. Analysis by HPLC and LC-UV/MS revealed the formation of only one major metabolite, which had a shorter retention time than **PT638** and which co-eluted with amino analogue **PT662** (Figure 4B). LC-MS showed that this metabolite had a mass of 305.0771, which corresponds to the molecular ion of **PT662** (Figure 4C). These results indicate that **PT638** was metabolized to **PT662** by MRSA cell lysate.

Because NfsA and NfsB are the two major nitroreductases in bacteria,³⁵ these enzymes were cloned and purified from MRSA, and their catalytic activities toward **PT638** were assayed using NADH or NADPH as the co-substrate (Figure S4). **PT638** was found to be a substrate for both nitroreductases but was reduced much more effectively by NfsB than by NfsA, with k_{cat}/K_m values of 1.0×10^6 and $5.2 \times 10^4 \text{ M}^{-1}\text{s}^{-1}$, respectively (Table 3). Finally, although **PT638** did not inhibit saLeuRS, amino analogue **PT662** had an IC_{50} value of $3.0 \mu\text{M}$ (Table 1). Thus, we propose that **PT638** is converted into an active saLeuRS inhibitor in MRSA cells primarily by the action of NfsB.

Other antibacterial prodrugs have been discovered such as nitrofurantoin,³² mentioned above, and the anti-tuberculosis nitroimidazole PA-824.³⁶ In these cases, antibacterial

activity is due to reactive intermediates, such as NO in the case of PA-824, formed during reduction of the nitro group that likely have multiple targets in the cell, and selection for resistance results in mutations in the enzymes responsible for prodrug activation including *nfsA* and *nfsB* for nitrofurantoin and a deazaflavin-dependent nitroreductase Ddn for PA-824.³⁷ In contrast, no mutations were observed in *nfsA* and *nfsB* when selecting for resistance to **PT638** but in the LeuRS target, supporting a specific mode of action in which reactive intermediates are not formed and in which mutations in the primary target are sufficient for resistance. In this regard, we note that the MIC of the ortho-nitro analog **PT659** is ~ 10-fold higher than that of **PT638** (MIC 0.4 and 6.25 µg/mL, respectively, Table 1) and the IC₅₀ value for inhibition of saLeuRS is reported to be ~10-fold greater for the corresponding amines in Xia et al.²⁵ (IC₅₀ 1.9 and 15.4 µM, respectively). The 8-fold increase in antibacterial of **PT638** compared to the aniline **PT662** (MIC 0.4 and 3.1 µg/mL, respectively) is thus likely because the former is better at penetrating the bacterial cells and accumulates following activation. However, although **PT662** is the only stable metabolite formed during activation of **PT638**, we cannot rule out the possibility that the activity of **PT638** might partially be due to one or more reactive intermediates formed during bioactivation of **PT638**.

Conclusion

LeuRS is a common target for the oxaborole class of compounds, which inhibit this enzyme by forming an adduct with the terminal adenosine of the bound tRNA substrate. In an attempt to identify additional antibacterial targets for the oxaboroles, we selected the nitrophenylsulfonamide-substituted benzoxaborole **PT638** as a probe for mode of action studies on the basis of reports that it has potent antibacterial activity toward *S. aureus* but did not inhibit LeuRS. We confirmed the antibacterial activity of **PT638** toward MRSA (MIC = 0.4 µg/mL) and then synthesized a series of 6-substituted benzoxaborole analogues for SAR studies. These studies showed that the nitro group, the sulfonamide linker, and oxaborole ring were all important for antibacterial activity and that any modification of the nitro group led to at least a 4-fold increase in the MIC relative to that of the parent compound. Although a LeuRS aminoacylation assay confirmed that **PT638** did not inhibit saLeuRS, selection for resistance to **PT638** and subsequent whole genome sequencing revealed mutations in the editing domain of saLeuRS. Bacterial cell lysate was found to convert **PT638** into amino analogue **PT662**, which inhibited saLeuRS with an IC₅₀ of 3 µM. In addition, **PT638** was shown to be a substrate for the bacterial nitroreductase enzymes NfsA and NfsB, confirming that the nitro analogue is a prodrug that is reduced into the active pharmacophore in bacterial cells.

Materials and Methods

Antibacterial activity

Minimum inhibitor concentrations (MICs) were determined using MRSA strain ATCC BAA-1762. Bacteria were cultured to mid-log phase (OD₆₀₀ = 0.6, 10⁸ cfu/mL) in cation-adjusted Mueller–Hinton (CAMH) medium at 37 °C in an orbital shaker. An inoculum of 10⁶ cells per well was placed in transparent 96-well plates and treated with inhibitor at final

concentrations ranging from 0.2 to 100 µg/mL. The MIC was defined as the minimum concentration at which a well showed no obvious growth by visual inspection.

Time-kill experiments

MRSA (ATCC BAA-1762) was grown in CAMH medium to mid-log phase ($OD_{600} = 0.6$, 10^8 cfu/mL) at 37 °C in a shaker and then diluted 100-fold into fresh medium. **PT638** or an equal volume of vehicle (DMSO) was then added to give concentrations 1, 4, or 16 times the MIC. Cultures were then shaken at 37 °C for 8 h. Kill curves were obtained by sampling the cell cultures at various times and plating serial dilutions on Mueller–Hinton agar. Colony forming units (cfus) were counted after incubation of the plates overnight at 37 °C. Each experiment was repeated at least twice.

Post-antibiotic effect

MRSA (ATCC BAA-1762) was grown in CAMH medium to mid-log phase ($OD_{600} = 0.6$, 10^8 cfu/mL) at 37 °C in a shaker and diluted 100-fold into fresh medium containing either **PT638** or an equal volume of DMSO. After the culture was shaken for 1 h at 37 °C, **PT638** was washed out by diluting the culture 1000-fold into fresh CAMH medium. The diluted cells were incubated in a shaker at 37 °C for an additional 5 h. The regrowth of MRSA cells was monitored by taking 100 µL of cell culture per hour and plating serial dilutions on Mueller–Hinton agar plates. The plates were incubated at 37 °C overnight, after which cfus were counted. The post-antibiotic effect was calculated as the time difference required for the number of compound-treated cells (cfus) to increase 1 log compared to the number of untreated cells. Each experiment was repeated in triplicate.

Generation of PT638-resistant strains and whole genome sequencing

MRSA (ATCC BAA-1762) was grown in CAMH medium to a cell density of 10^9 cfu/mL and then 100 µL of the cell culture was plated on Mueller–Hinton agar containing **PT638** (4 µg/mL, $10 \times$ MIC). After incubation at 37 °C for 48 h, three colonies were picked, and the genomic DNA was purified using a GenElute Bacterial Genomic DNA Kit (Sigma). Whole genome sequencing was performed by Admera Health.

Cloning, expression, and purification of saLeuRS

The *leuRS* gene from MRSA cells (ATCC BAA-1762) was amplified with primers 5'CGCGGATCCGTGTTGAATTACAACCACAATC3' and 5'CCGCTCGAGTTATTTAGCTACAATATTGAC3'. The amplified *leuRS* gene was cloned into a pET28a vector so that a His-tag was encoded at the N-terminus of the protein. After sequencing, the pET28a-leuRS plasmid was transformed into *E. coli* BL21(DE3) cells, which were then grown overnight in 10 mL of Luria-Bertani (LB) medium containing 50 µg/mL kanamycin. Then the overnight culture was inoculated into 1 L of LB medium containing kanamycin at the same concentration, and the cells were grown until the OD_{600} reached 0.6. One mM Isopropyl β-D-1-thiogalactopyranoside (IPTG) was added to induce protein expression, and the culture was shaken overnight at 20 °C. Cells were harvested by centrifugation at 5000 rpm for 10 min at 4 °C. The cell pellet was resuspended in 30 mL of His-binding buffer (50 mM Tris-HCl, 150 mM NaCl, 5 mM Imidazole, pH 7.9), and the

bacteria were disrupted by sonication. Cell debris was removed by centrifugation at 40,000 rpm for 60 min at 4 °C, and the clear supernatant was loaded onto a His-bind column (1.5 cm × 15 cm) containing 4 mL of His-bind resin (Novagen) that had been charged with 10 mL of charge buffer (Ni²⁺). The column was washed with wash buffer containing 60 mM imidazole, and the protein was eluted from the column with elution buffer containing 500 mM imidazole. Fractions containing protein were loaded onto a size-exclusion column (Superdex 75, GE Healthcare) and eluted with 60 mM 4-(2-hydroxyethyl)-1-piperazineethanesulfonic acid (HEPES) buffer (pH 8.0) containing 30 mM NaCl and 30 mM MgCl₂ to remove imidazole.

LeuRS aminoacylation activity assay

The aminoacylation reaction was performed in a 50 μL reaction volume with 7 nM saLeuRS, 15 μM *E. coli* total tRNA (Roche), 20 μM ³H-leucine (174.6 mCi/mmol), and 4 mM ATP in 50 mM HEPES-KOH buffer (pH 8.0) containing 30 mM MgCl₂, 30 mM KCl, 0.02% (w/v) bovine serum albumin, and 1 mM dithiothreitol. Unless stated otherwise, the test compound, saLeuRS, and *E. coli* total tRNA were pre-incubated for 20 min before the reaction was initiated with 4 mM ATP. At specific times, tRNA was precipitated by the addition of 10% (w/v) trichloroacetic acid. The precipitate was collected with a 0.45 μm microcentrifugal filter (Thomas Scientific F2517-2) and washed twice with 100 μL of 5% trichloroacetic acid, and then the filter was counted with a liquid scintillation analyzer (Tri-Carb 2900TR, PerkinElmer).

IC₅₀ values were determined at various concentrations of compound (Figure S2) and data were fit to a 4 parameter IC₅₀ equation in GraphPad Prism 4 after constraining the Hill slope to a value of 1. Each experiment was performed in triplicate.

Cytotoxicity

The in vitro cytotoxicity of **PT638** and **PT662** was determined using Vero cells (ATCC CCL-81). Cells were grown in Dulbecco's Modified Eagle Medium (DMEM) with 10% fetal bovine serum and then aliquoted into a 96-well tissue culture plate to give 2 × 10⁴ cells/well. After incubation for 24 h at 37 °C in 5% CO₂, the media was aspirated and replaced with serum-free DMEM. After an additional 1 h of incubation, **PT638** or **PT662** was added to give a final concentration ranging from 0.2 to 100 μg/mL. Following incubation for 24 h at 37 °C in 5% CO₂, cell viability was assessed by means of an MTT assay (Vybrant MTT Cell Proliferation Assay Kit). The absorbance of each well was measured at 570 nm and the data were used to determine compound cytotoxicity (IC₅₀).

Cloning, expression, and purification of NfsA and NfsB

The *nfsA* gene from MRSA (ATCC BAA-1762) was amplified with primers 5'CTAGCTAGCGTGTGTCAGATCATGTATATAATC3' and 5'CGCGGATCCCTATCGCTGTATTAAGCCTG3'. The *nfsB* gene from the same strain was amplified with 5'CTAGCTAGCATGAGCAATATGAATCAAACAATTATG3' and 5'CGCGGATCCTTATTCTTTTGGTCCAACCC3'. The amplified *nfsA* (*nfsB*) gene was cloned into a pET28a vector so that a His-tag was encoded at the N-terminus of the protein. After sequencing, the pET28a-*nfsA* (pET28a-*nfsB*) plasmid was transformed into *E. coli*

BL21(DE3) cells, which were then grown overnight in 10 mL of LB medium containing 50 µg/mL kanamycin. Then the overnight culture was inoculated into 1 L of LB medium containing kanamycin at the same concentration, and the cells were grown until the OD₆₀₀ reached 0.6. IPTG (1 mM) was added to induce protein expression, and the culture was shaken overnight at 20 °C. Cells were harvested by centrifugation at 5000 rpm for 10 min at 4 °C. The cell pellet was resuspended in 30 mL of His-binding buffer (50 mM Tris-HCl, 150 mM NaCl, 5 mM imidazole, pH 7.4), and the bacteria were disrupted by sonication. Cell debris was removed by centrifugation at 40,000 rpm for 60 min at 4 °C, and the clear supernatant was loaded onto a His-bind column (1.5 cm × 15 cm) containing 4 mL of His-bind resin (Novagen) that had been charged with 10 mL of charge buffer (Ni²⁺). The column was washed with washing buffer containing 30 mM imidazole, and the protein was eluted from the column with elution buffer containing 500 mM imidazole. Fractions containing protein were loaded onto a size-exclusion column (Superdex 75, GE Healthcare), which was eluted with 50 mM Tris-HCl buffer (pH 7.4) containing 150 mM NaCl to remove the imidazole. The concentrations of NfsA and NfsB were determined from the flavin absorbance at 450 nm.

Nitroreductase activity assay

The nitroreductase assay was performed in 50 mM Tris-HCl buffer (pH 7.4), containing 5 mM EDTA at RT in a total reaction volume of 500 µL. Reactions were initiated by the addition of NfsA or NfsB to a final concentration of 45 nM and the consumption of NAD(P)H was continuously monitored at 340 nm. The k_{cat} and K_{m} values were determined at a fixed concentration of NAD(P)H (60 µM NADPH for NfsA, 60 µM NADH for NfsB) and by varying the concentration of **PT638** (6.25–1500 µM). Initial velocities as a function of substrate concentration were fit to the Michaelis–Menten equation using GraphPad Prism 4. Each experiment was performed for triplicate.

PT638 metabolite analysis

MRSA (ATCC BAA-1762) was grown in 20 mL of CAMH medium to log phase (OD₆₀₀ = 0.6). Cells were harvested by centrifugation and then resuspended in 5 mL of lysis buffer (50 mM Tris-HCl, 100 mM NaCl, pH 8.0). Cells were lysed by sonication, and cell debris was removed by centrifugation. The supernatant was then incubated with 4 µg/mL **PT638** at 37 °C. After 3, 24, and 48 h, 500 µL of cell lysate was removed and extracted twice with ethyl acetate. The organic layers were combined, and the solvent was removed by rotary evaporation. The residue after rotovapping was then dissolved in 300 µL of 50% MeCN/H₂O and analyzed by HPLC with a Phenomenex C18 column (250 × 4.6 mm). A linear gradient at a flow rate of 0.8 mL/min was used, with absorbance detection at 254 nm. Solvent A was water, and solvent B was acetonitrile. The percentages of solvent B at times t were as follow: $t = 0\text{--}5$ min, B = 5%; $t = 5\text{--}35$ min, B = 5–100%; $t = 35\text{--}40$ min, B = 100%; $t = 40\text{--}50$ min, B = 100–5%; $t = 50\text{--}55$ min, B = 5%.

The sample taken at 48 h was also analyzed by LC-MS using an Agilent LC-UV-TOF system consisting of a 1260 uPLC, a UV–vis diode-array detector, and a TOF mass analyzer. The LC eluent consisted of a gradient of solvent A (water with 0.1% formic acid) and solvent B (acetonitrile). The percentages of solvent B at times t were as follows: $t = 0\text{--}1$ min,

B = 5%; $t = 1\text{--}31$ min, B = 5–95%; $t = 31\text{--}33$ min, B = 95–99%. Compounds were detected by monitoring absorbance at 287 nm. Mass data were collected with an in-line mass spectrometer (G6224A oaTOF) in positive-ion mode.

Supplementary Material

Refer to Web version on PubMed Central for supplementary material.

Acknowledgements

This work was supported by NIH grants GM102864 and AI119316 to PJT and GM092714 to JI (T32 Fellowship). We thank Dr. Bela Ruzsicska for his help with LC-UV/MS and high-resolution MS.

References

- (1). Karras G; Giannakaki V; Kotsis V; Miyakis S (2012) Novel antimicrobial agents against multi-drug-resistant gram-negative bacteria: an overview *Recent Pat Antiinfect Drug Discov*, 7, 175–81. DOI: 10.2174/157489112803521922 [PubMed: 23061790]
- (2). Giannakaki V; Miyakis S (2012) Novel antimicrobial agents against multi-drug-resistant gram-positive bacteria: an overview *Recent Pat Antiinfect Drug Discov*, 7, 182–8. DOI: 10.2174/157489112803521959 [PubMed: 23016758]
- (3). Santajit S; Indrawattana N (2016) Mechanisms of Antimicrobial Resistance in ESKAPE Pathogens *Biomed Res Int*, 2016, 2475067 DOI: 10.1155/2016/2475067 [PubMed: 27274985]
- (4). Mathur P; Singh S (2013) Multidrug resistance in bacteria: a serious patient safety challenge for India *J Lab Physicians*, 5, 5–10. DOI: 10.4103/0974-2727.115898 [PubMed: 24014960]
- (5). Fisher JF; Meroueh SO; Mobashery S (2005) Bacterial resistance to beta-lactam antibiotics: compelling opportunism, compelling opportunity *Chem Rev*, 105, 395–424. DOI: 10.1021/cr030102i [PubMed: 15700950]
- (6). Theuretzbacher U (2013) Global antibacterial resistance: The never-ending story *J Glob Antimicrob Resist*, 1, 63–69. DOI: 10.1016/j.jgar.2013.03.010 [PubMed: 27873580]
- (7). Xia Y; Cao K; Zhou Y; Alley MR; Rock F; Mohan M; Meewan M; Baker SJ; Lux S; Ding CZ; Jia G; Kully M; Plattner JJ (2011) Synthesis and SAR of novel benzoxaboroles as a new class of beta-lactamase inhibitors *Bioorg Med Chem Lett*, 21, 2533–6. DOI: 10.1016/j.bmcl.2011.02.024 [PubMed: 21392987]
- (8). Dong C; Virtucio C; Zemska O; Baltazar G; Zhou Y; Baia D; Jones-Iatauro S; Sexton H; Martin S; Dee J; Mak Y; Meewan M; Rock F; Akama T; Jarnagin K (2016) Treatment of Skin Inflammation with Benzoxaborole Phosphodiesterase Inhibitors: Selectivity, Cellular Activity, and Effect on Cytokines Associated with Skin Inflammation and Skin Architecture Changes *J Pharmacol Exp Ther*, 358, 413–22. DOI: 10.1124/jpet.116.232819 [PubMed: 27353073]
- (9). Akama T; Dong C; Virtucio C; Sullivan D; Zhou Y; Zhang YK; Rock F; Freund Y; Liu L; Bu W; Wu A; Fan XQ; Jarnagin K (2013) Linking phenotype to kinase: identification of a novel benzoxaborole hinge-binding motif for kinase inhibition and development of high-potency rho kinase inhibitors *J Pharmacol Exp Ther*, 347, 615–25. DOI: 10.1124/jpet.113.207662 [PubMed: 24049062]
- (10). Adamczyk-Wozniak A; Borys KM; Sporzynski A (2015) Recent developments in the chemistry and biological applications of benzoxaboroles *Chem Rev*, 115, 5224–47. DOI: 10.1021/cr500642d [PubMed: 26017806]
- (11). Rock FL; Mao W; Yaremchuk A; Tukalo M; Crepin T; Zhou H; Zhang YK; Hernandez V; Akama T; Baker SJ; Plattner JJ; Shapiro L; Martinis SA; Benkovic SJ; Cusack S; Alley MR (2007) An antifungal agent inhibits an aminoacyl-tRNA synthetase by trapping tRNA in the editing site *Science*, 316, 1759–61. DOI: 10.1126/science.1142189 [PubMed: 17588934]

- (12). Dowlut M; Hall DG (2006) An improved class of sugar-binding boronic acids, soluble and capable of complexing glycosides in neutral water J Am Chem Soc, 128, 4226–7. DOI: 10.1021/ja057798c [PubMed: 16568987]
- (13). Berube M; Dowlut M; Hall DG (2008) Benzoboroxoles as efficient glycopyranoside-binding agents in physiological conditions: Structure and selectivity of complex formation J Org Chem, 73, 6471–6479. DOI: 10.1021/jo800788s [PubMed: 18549270]
- (14). Rawat R; Whitty A; Tonge PJ (2003) The isoniazid-NAD adduct is a slow, tight-binding inhibitor of InhA, the *Mycobacterium tuberculosis* enoyl reductase: adduct affinity and drug resistance Proc Natl Acad Sci U S A, 100, 13881–13886. DOI: 10.1073/pnas.2235848100 [PubMed: 14623976]
- (15). Baldock C; Rafferty JB; Sedelnikova SE; Baker PJ; Stuitje AR; Slabas AR; Hawkes TR; Rice DW (1996) A mechanism of drug action revealed by structural studies of enoyl reductase Science, 274, 2107–2110. DOI: 10.1126/science.274.5295.2107 [PubMed: 8953047]
- (16). Sarkar J; Mao W; Lincecum TL Jr.; Alley MR; Martinis SA (2011) Characterization of benzoxaborole-based antifungal resistance mutations demonstrates that editing depends on electrostatic stabilization of the leucyl-tRNA synthetase editing cap FEBS Lett, 585, 2986–91. DOI: 10.1016/j.febslet.2011.08.010 [PubMed: 21856301]
- (17). Palencia A; Li X; Bu W; Choi W; Ding CZ; Easom EE; Feng L; Hernandez V; Houston P; Liu L; Meewan M; Mohan M; Rock FL; Sexton H; Zhang S; Zhou Y; Wan B; Wang Y; Franzblau SG; Woolhiser L; Gruppo V; Lenaerts AJ; O'Malley T; Parish T; Cooper CB; Waters MG; Ma Z; Ioeberger TR; Sacchetti JC; Rullas J; Angulo-Barturen I; Perez-Herran E; Mendoza A; Barros D; Cusack S; Plattner JJ; Alley MR (2016) Discovery of Novel Oral Protein Synthesis Inhibitors of *Mycobacterium tuberculosis* That Target Leucyl-tRNA Synthetase Antimicrob Agents Chemother, 60, 6271–80. DOI: 10.1128/AAC.01339-16 [PubMed: 27503647]
- (18). Sonoiki E; Palencia A; Guo D; Ahyong V; Dong C; Li X; Hernandez VS; Zhang YK; Choi W; Gut J; Legac J; Cooper R; Alley MR; Freund YR; DeRisi J; Cusack S; Rosenthal PJ (2016) Antimalarial Benzoxaboroles Target *Plasmodium falciparum* Leucyl-tRNA Synthetase Antimicrob Agents Chemother, 60, 4886–95. DOI: 10.1128/AAC.00820-16 [PubMed: 27270277]
- (19). Palencia A; Liu RJ; Lukarska M; Gut J; Bougdour A; Touquet B; Wang ED; Li X; Alley MR; Freund YR; Rosenthal PJ; Hakimi MA; Cusack S (2016) *Cryptosporidium* and *Toxoplasma* Parasites Are Inhibited by a Benzoxaborole Targeting Leucyl-tRNA Synthetase Antimicrob Agents Chemother, 60, 5817–27. DOI: 10.1128/AAC.00873-16 [PubMed: 27431220]
- (20). Monteferrante CG; Jirgensons A; Varik V; Hauriuk V; Goessens WH; Hays JP (2016) Evaluation of the characteristics of leucyl-tRNA synthetase (LeuRS) inhibitor AN3365 in combination with different antibiotic classes Eur J Clin Microbiol Infect Dis, 35, 1857–1864. DOI: 10.1007/s10096-016-2738-1 [PubMed: 27506217]
- (21). Mendes RE; Alley MR; Sader HS; Biedenbach DJ; Jones RN (2013) Potency and spectrum of activity of AN3365, a novel boron-containing protein synthesis inhibitor, tested against clinical isolates of Enterobacteriaceae and nonfermentative Gram-negative bacilli Antimicrob Agents Chemother, 57, 2849–57. DOI: 10.1128/AAC.00160-13 [PubMed: 23507283]
- (22). Hernandez V; Crepin T; Palencia A; Cusack S; Akama T; Baker SJ; Bu W; Feng L; Freund YR; Liu L; Meewan M; Mohan M; Mao W; Rock FL; Sexton H; Sheoran A; Zhang Y; Zhang YK; Zhou Y; Nieman JA; Anugula MR; Keramane el M; Savariraj K; Reddy DS; Sharma R; Subedi R; Singh R; O'Leary A; Simon NL; De Marsh PL; Mushtaq S; Warner M; Livermore DM; Alley MR; Plattner JJ (2013) Discovery of a Novel Class of Boron-Based Antibacterials with Activity against Gram-Negative Bacteria Antimicrob Agents Chemother, 57, 1394–403. DOI: 10.1128/AAC.02058-12 [PubMed: 23295920]
- (23). O'Dwyer K; Spivak AT; Ingraham K; Min S; Holmes DJ; Jakielaszek C; Rittenhouse S; Kwan AL; Livi GP; Sathe G; Thomas E; Van Horn S; Miller LA; Twynholm M; Tomayko J; Dalessandro M; Caltabiano M; Scangarella-Oman NE; Brown JR (2015) Bacterial Resistance to Leucyl-tRNA Synthetase Inhibitor GSK2251052 Develops during Treatment of Complicated Urinary Tract Infections Antimicrob Agents Chemother, 59, 289–98. DOI: 10.1128/AAC.03774-14 [PubMed: 25348524]

- (24). Zhao H; Palencia A; Seiradake E; Ghaemi Z; Cusack S; Luthey-Schulten Z; Martinis S (2015) Analysis of the Resistance Mechanism of a Benzoxaborole Inhibitor Reveals Insight into the Leucyl-tRNA Synthetase Editing Mechanism *ACS Chem Biol*, 10, 2277–85. DOI: 10.1021/acschembio.5b00291 [PubMed: 26172575]
- (25). Xia Y; Alley MKR; Zhou Y; Hernandez VS; Plattner JJ; Ding CZ; Cao K; Zhang YK; Benowitz A; Akama T; Sligar J; Jia G; Ou L; Saraswat N; Ramachandran S; Diaper C; Zhang Y; Banda GR; Nieman JA; Keramane M; Mohammed R; Subedi R; Liang H; Singh R (2010) Boron-containing small molecules, US 2010.0256092A1
- (26). Petersen PJ; Jones CH; Bradford PA (2007) In vitro antibacterial activities of tigecycline and comparative agents by time-kill kinetic studies in fresh Mueller-Hinton broth *Diagn Microbiol Infect Dis*, 59, 347–9. DOI: 10.1016/j.diagmicrobio.2007.05.013 [PubMed: 17662552]
- (27). Silva F; Lourenco O; Queiroz JA; Domingues FC (2011) Bacteriostatic versus bactericidal activity of ciprofloxacin in *Escherichia coli* assessed by flow cytometry using a novel far-red dye *J Antibiot (Tokyo)*, 64, 321–5. DOI: 10.1038/ja.2011.5 [PubMed: 21326251]
- (28). Pankey GA; Sabath LD (2004) Clinical relevance of bacteriostatic versus bactericidal mechanisms of action in the treatment of Gram-positive bacterial infections *Clin Infect Dis*, 38, 864–70. DOI: 10.1086/381972 [PubMed: 14999632]
- (29). Hu QH; Liu RJ; Fang ZP; Zhang J; Ding YY; Tan M; Wang M; Pan W; Zhou HC; Wang ED (2013) Discovery of a potent benzoxaborole-based anti-pneumococcal agent targeting leucyl-tRNA synthetase *Sci Rep*, 3, 2475 DOI: 10.1038/srep02475 [PubMed: 23959225]
- (30). Palencia A; Crepin T; Vu MT; Lincecum TL Jr.; Martinis SA; Cusack S (2012) Structural dynamics of the aminoacylation and proofreading functional cycle of bacterial leucyl-tRNA synthetase *Nat Struct Mol Biol*, 19, 677–84. DOI: 10.1038/nsmb.2317 [PubMed: 22683997]
- (31). Whiteway J; Koziazar P; Veall J; Sandhu N; Kumar P; Hoecher B; Lambert IB (1998) Oxygen-insensitive nitroreductases: analysis of the roles of *nfsA* and *nfsB* in development of resistance to 5-nitrofurantoin derivatives in *Escherichia coli* *J Bacteriol*, 180, 5529–39. [PubMed: 9791100]
- (32). Sandegren L; Lindqvist A; Kahlmeter G; Andersson DI (2008) Nitrofurantoin resistance mechanism and fitness cost in *Escherichia coli* *J Antimicrob Chemother*, 62, 495–503. DOI: 10.1093/jac/dkn222 [PubMed: 18544599]
- (33). Patterson S; Wyllie S (2014) Nitro drugs for the treatment of trypanosomatid diseases: past, present, and future prospects *Trends Parasitol*, 30, 289–98. DOI: 10.1016/j.pt.2014.04.003 [PubMed: 24776300]
- (34). Miller AF; Park JT; Ferguson KL; Pitsawong W; Bommarius AS (2018) Informing Efforts to Develop Nitroreductase for Amine Production Molecules, 23 DOI: 10.3390/molecules23020211
- (35). Tavares AF; Nobre LS; Melo AM; Saraiva LM (2009) A novel nitroreductase of *Staphylococcus aureus* with S-nitrosoglutathione reductase activity *J Bacteriol*, 191, 3403–6. DOI: 10.1128/JB.00022-09 [PubMed: 19286809]
- (36). Manjunatha U; Boshoff HI; Barry CE (2009) The mechanism of action of PA-824: Novel insights from transcriptional profiling *Commun Integr Biol*, 2, 215–8. DOI: 10.4161/cib.2.3.7926 [PubMed: 19641733]
- (37). Manjunatha UH; Boshoff H; Dowd CS; Zhang L; Albert TJ; Norton JE; Daniels L; Dick T; Pang SS; Barry CE 3rd. (2006) Identification of a nitroimidazo-oxazine-specific protein involved in PA-824 resistance in *Mycobacterium tuberculosis* *Proc Natl Acad Sci U S A*, 103, 431–6. DOI: 10.1073/pnas.0508392103 [PubMed: 16387854]

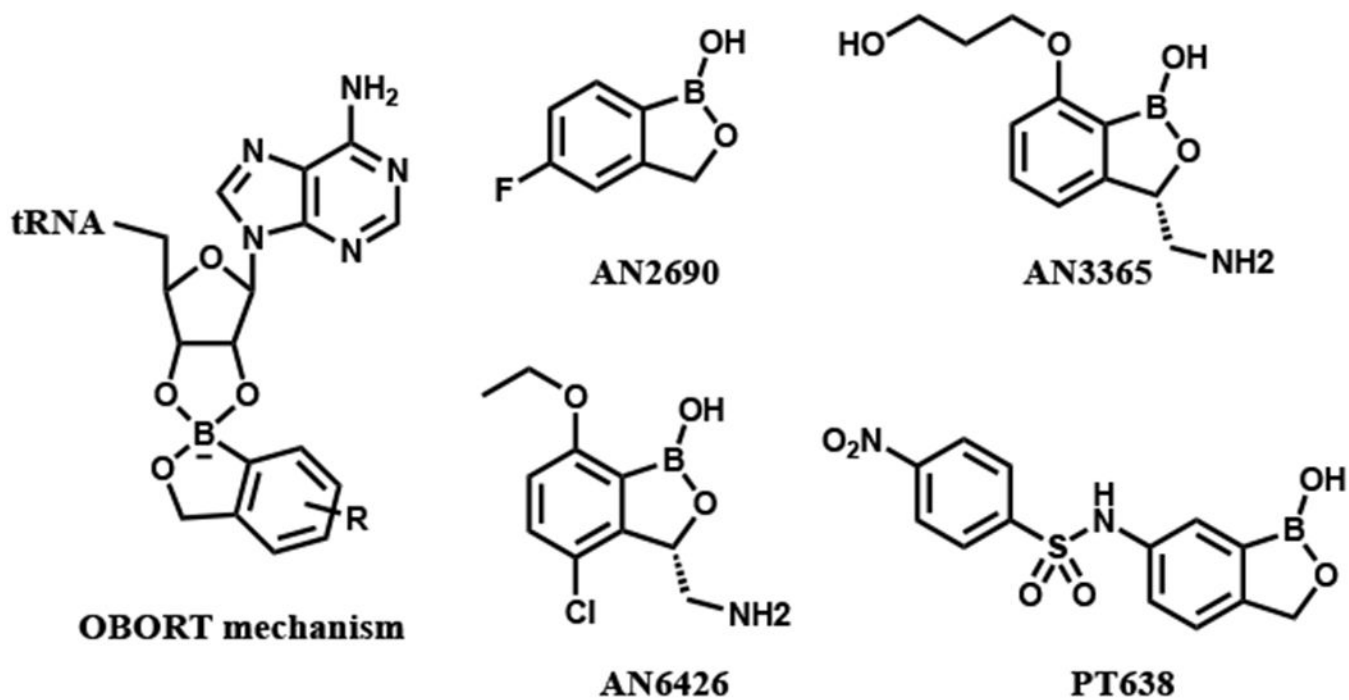


Figure 1.
OBORT mechanism and oxaborole-based enzyme inhibitors.

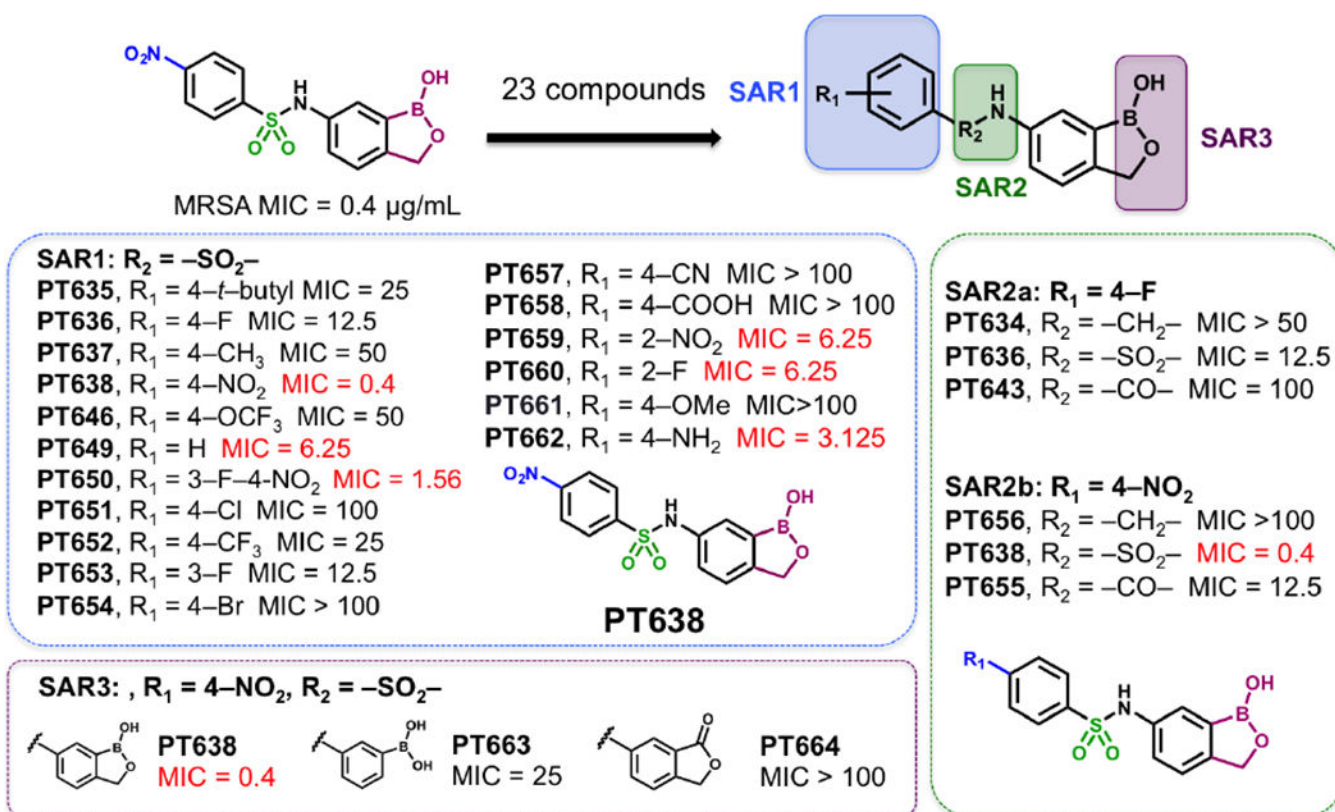


Figure 2. Structure–activity relationships (SARs) for inhibition of bacterial growth.

Three series of analogues were synthesized to explore SAR associated with the substituent on the phenyl ring (SAR1), the sulfonamide linker (SAR2), and the oxaborole ring (SAR3). MIC values (µg/mL) against MRSA (ATCC BAA-1762) were determined by broth microdilution; values of < 10 µg/mL are indicated in red.

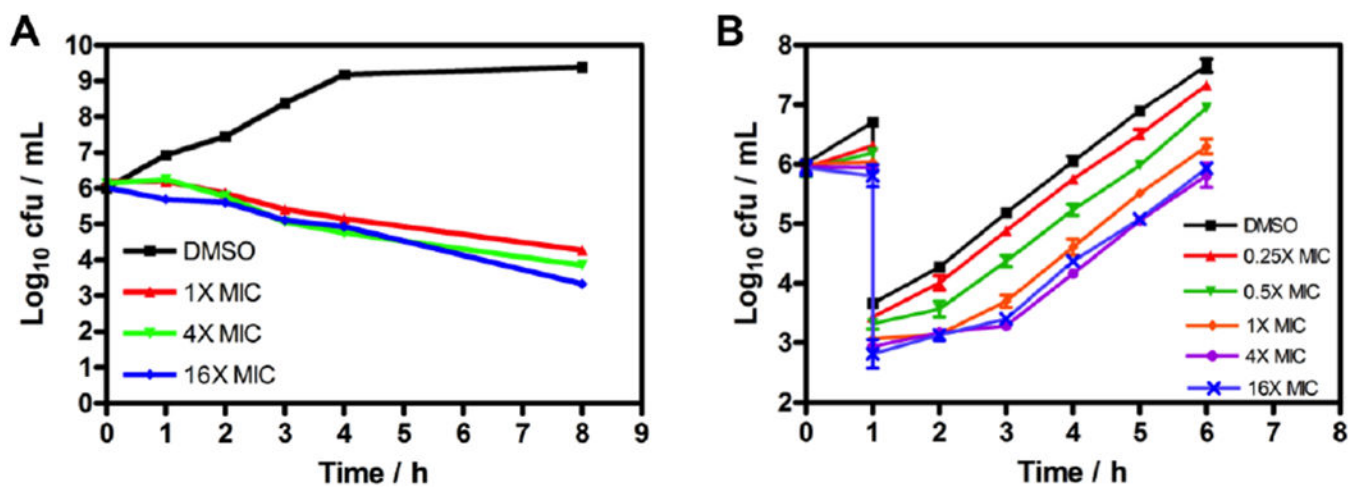


Figure 3. Time-kill experiments and post-antibiotic effect of PT638.

(A) Cell viability of MRSA (ATCC BAA-1762) treated with **PT638** at 1, 4, and 16 times the MIC or with vehicle (DMSO) over the course of 8 h. (B) Post-antibiotic effect of **PT638**.

Recovery of bacterial growth was measured after 1 h of exposure to **PT638** at 0.25, 0.5, 1, 4, and 16 times the MIC and subsequent washout. Values are means of three independent replicates, and error bars indicate the standard deviations.

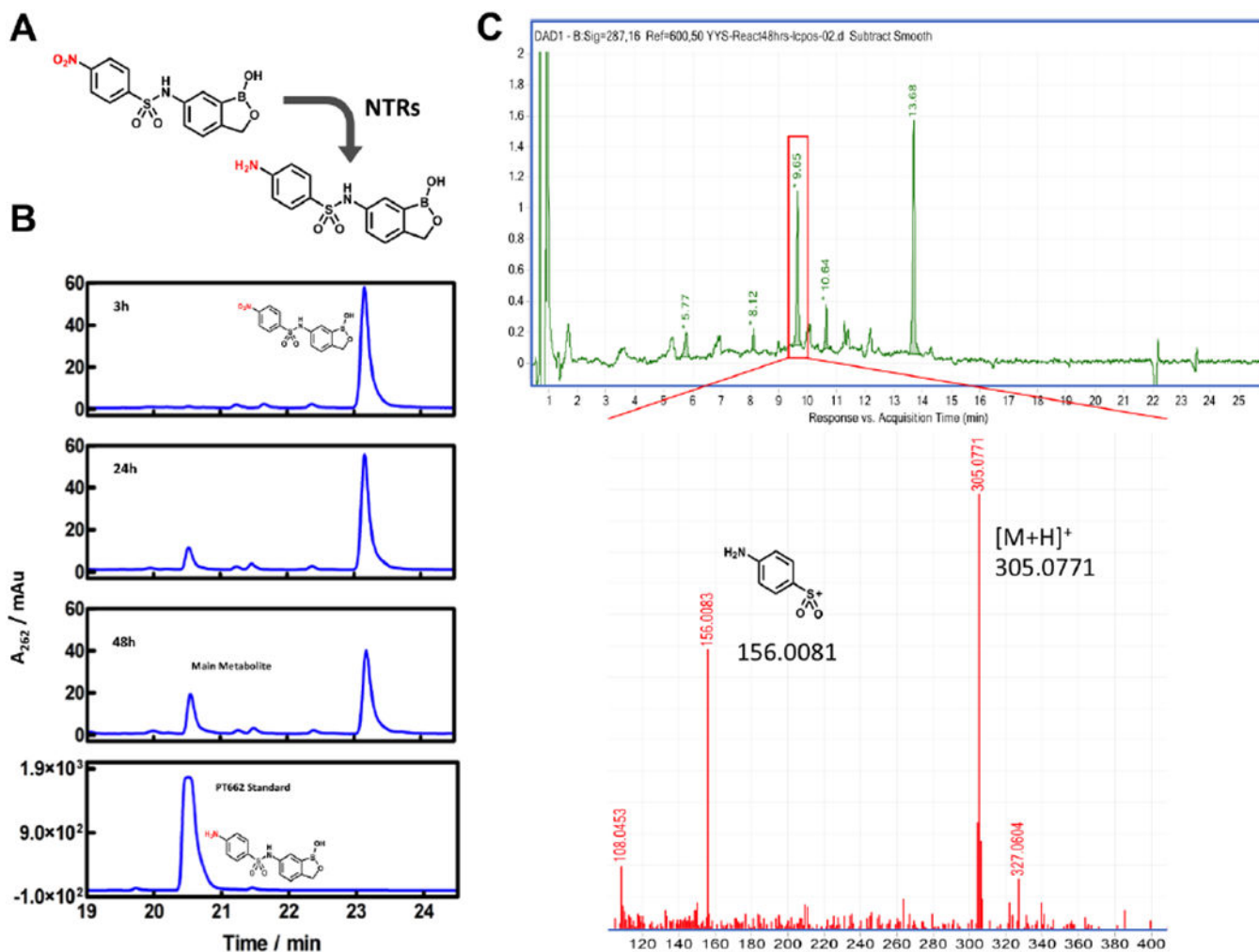
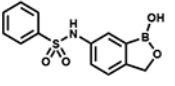
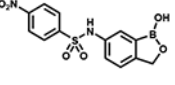
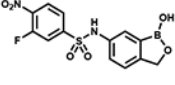
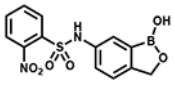
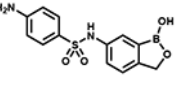
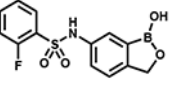


Figure 4. Formation of PT662 in MRSA cell lysate treated with PT638.

(A) Reduction of **PT638** to aniline **PT662** by nitroreductases in MRSA cells. (B) HPLC analysis of **PT638** metabolites extracted from MRSA cell lysate at 3, 24, and 48 h. **PT638** had a retention time of 23.2 min, and the major metabolite had a retention time of 20.7 min, which was identical to that of synthetic **PT662** standard. (C) High-resolution LC-UV/MS spectra of sample obtained after incubation for 48 h. The major metabolite had a retention time of 9.65 min with $[M + H]^+ = 305.0771$ and $m/z = 156.0081$. NTRs, nitroreductases.

Table 1.

Biochemical activities of oxaboroles with MIC values <10 µg/mL

Compound	Structure	IC ₅₀ (µM) ^a	MIC ^b MRSA (µg/mL)	Cytotoxicity ^c Vero cells (IC ₅₀ µg/mL)
PT649		94 ± 2	6.25	N.D.
PT638		>100	0.4	100
PT650		>100	1.56	N.D.
PT659		>100	6.25	N.D.
PT662		3.0 ± 1.2	3.125	100
PT660		28 ± 1	6.25	N.D.

^aIC₅₀ values were measured by means of a radiolabeled LeuRS aminoacylation assay.

^bMIC against MRSA ATCC BAA-1762 was determined using a broth microdilution method.

^cCytotoxicity was determined with Vero cells using an MTT cell viability assay. All measurements were performed in triplicate and standard errors are reported.

N.D., not determined.

Table 2.

PT63-resistant mutant stains

Strain	MIC shift ^a	Mutation	Protein
1	16-fold	D343Y	
2	8-fold	G303S	saLeuRS editing domain
3	8-fold	F233I	

^aThe MIC shift was determined from the MIC of the mutant strain compared to that of the wild-type MRSA strain (ATCC BAA-1762).

Author Manuscript

Author Manuscript

Author Manuscript

Author Manuscript

Table 3.Reduction of PT638 by NfsA and NfsB^a

Enzyme	k_{cat} (s ⁻¹)	K_m (μM)	k_{cat}/K_m (M ⁻¹ s ⁻¹)
NfsA	43.8±7.0	840±260	5.2×10 ⁴
NfsB	45.3±0.9	45±3	1×10 ⁶

^aInitial velocities were monitored at 340 nm at a fixed concentration of NAD(P)H (60 μM NADPH for NfsA, 60 μM NADH for NfsB) and varied concentrations of **PT638** (6.25–1500 μM). Data were fit to the Michaelis–Menten equation.